

Infrared Spectroscopic Observation and Characterization of Surface Ethylidyne on Supported Palladium on Alumina

T. P. BEEBE, JR., M. R. ALBERT, AND J. T. YATES, JR.

Surface Science Center, Department of Chemistry, University of Pittsburgh, Pittsburgh, Pennsylvania 15260

Received February 26, 1985; revised June 14, 1985

The first detailed characterization of the surface ethylidyne species adsorbed on a *supported transition metal surface*, namely, Pd/Al₂O₃ (10%) is reported. Upon addition of C₂H₄ or C₂H₂ to Pd/Al₂O₃ at 300 K, there is an immediate irreversible formation of surface ethylidyne ($\geq\text{C}-\text{CH}_3$), as evidenced by the development of three characteristic bands in the infrared spectrum [$\delta_s(\text{CH}_3) = 1333 \text{ cm}^{-1}$, $\nu(\text{C}-\text{C}) = 1088 \text{ cm}^{-1}$, and $\nu_s(\text{CH}_3) = 2867 \text{ cm}^{-1}$]. This assignment is further supported by H—D exchange experiments involving chemisorbed ethylidyne which correlate with analogous experiments on Rh(111). Thermal conversion from ethylene adsorbed at low temperatures to surface ethylidyne begins at $\approx 240 \text{ K}$; the surface ethylidyne species is stable up to about 400 K. These vibrational data, as well as the thermal stability data, are in excellent agreement with previous results on the Pd(111) and Rh(111) single-crystal surfaces. © 1985 Academic Press, Inc.

I. INTRODUCTION

There has been a great deal of work done in recent years characterizing and studying the chemisorbed ethylidyne species ($\geq\text{CCH}_3$). All of the work reported to date in the literature on the chemisorbed ethylidyne species has been done on the surface of single crystals in UHV (1-26). Although there has been some speculation concerning the role, if any, of the ethylidyne species in the mechanism of the hydrogenation reaction, as of yet no detailed measurements of the properties of surface ethylidyne have been made in any system other than in the highly controlled environment of single-crystal surface science research. This paper reports the first detailed characterization and measurements of the properties of ethylidyne on a palladium surface supported on alumina, a system similar to the catalysts used industrially in hydrogenation reactions.

The initial studies were conducted on Pt(111) (1-7), and have since been extended to Rh(111) (8, 13, 16, 24) and Pd(111) (12, 13, 17-19) surfaces. The initial characterization of the stable surface species formed upon addition of C₂H₂ or C₂H₄

to these surfaces at 300 K had originally generated considerable controversy, since there were no less than five surface structures proposed by various workers (25). It is now generally accepted that the surface structure is that of ethylidyne ($\geq\text{C}-\text{CH}_3$) (13).

The earliest structural studies were carried out by Kesmodel *et al.* (1), using LEED. They concluded that on Pt(111) acetylene formed a stable C₂H₂ di- σ bound species. This was soon followed by a UPS study (2), in which it was concluded that the stable species on Pt(111) and Pd(111) was an *sp*²-hybridized HC—CH species. The EELS study of Ibach *et al.* (3) on Pt(111) was the first of its kind involving C₂H₄ adsorption; here the ethylidene structure, >CHCH_3 , was proposed. The spectra were compared with the known vibrational spectra of CHCl₂CH₃ (4), giving only fair agreement.

Ibach's proposal of the ethylidene structure (3, 4) prompted Kesmodel *et al.* to reinvestigate their LEED data, considering new geometries in which the C—C bond is not necessarily parallel to the surface. This study (5, 6) led to the proposal of the ethylidyne structure which is now generally ac-

cepted. The new LEED calculations showed that the C—C bond was normal to the surface with a bond length of 1.5 Å, and that three equivalent Pt—C bonds form in a three-fold hollow site on the Pt(111) surface. Furthermore, it was shown that Ibach's EELS data (3, 4) was consistent with the ethylidyne structure based on vibrational data from analogous transition metal clusters containing ethylidyne ligands.

The next important contributions came from a photoemission study by Demuth (7) in which vinylidene ($-\text{CH}=\text{CH}_2$) was the stable species proposed. Through the use of TPD methods, a carbon-hydrogen stoichiometry of C_2H_3 was demonstrated (7). Albert *et al.* (14) in an ARUPS study using synchrotron radiation, determined that the C—C bond axis of the species on Pt(111) was normal to the surface and had orbitals with a symmetry consistent with an ethylidyne structure. Dubois *et al.* reported the same LEED, TPD, and EELS results on Rh(111) as on Pt(111) surfaces (8). This was the first indication that ethylidyne can exist on surfaces other than Pt(111).

An important TPD result from Steininger *et al.* (15) showed that the amount of H_2 evolved during conversion of C_2H_4 to the stable surface species, compared with the total amount of H_2 evolved through decomposition is one to four. This result, in conjunction with Demuth's TPD stoichiometry of C_2H_3 (7), provided strong quantitative evidence that C_2H_4 converts to $\text{>C}-\text{CH}_3$ (ethylidyne) and not CHCH_3 (ethylidene).

Skinner *et al.* (11) reported a complete normal mode analysis, along with vibrational mode assignments for the ethylidyne nonacarbonyl tricobalt complex $\text{CH}_3\text{CCO}_3(\text{CO})_9$. Comparison of the normal mode analysis with the EELS data of the ethylidyne surface species gave an excellent agreement of the relative peak intensities and wavenumber positions and has provided convincing evidence that the ethylidyne species is the stable product

from C_2H_4 decomposition on Pt(111) and Rh(111).

More recently, Kesmodel and Gates (12, 17, 19) have shown that the ethylidyne species is also produced from $\text{C}_2\text{H}_2 + \text{H}_2$, and from C_2H_4 adsorption on the Pd(111) crystal face. In addition, the symmetry of the various modes was investigated using off-specular scattering in EELS, and it was shown that both the C—C stretch mode and the symmetric methyl deformation mode are associated with a dipole derivative component that lies perpendicular to the surface. These conclusions are in exact agreement with the conclusions of Skinner *et al.* on the structure of the ethylidyne transition metal complex (11, 12). Koestner *et al.* (16) determined from LEED measurements that on Rh(111) the C—C bond of ethylidyne is anomalously short for an sp^3 carbon (1.45 ± 0.10 Å vs 1.54 Å); it was proposed that the ethylidyne orbitals undergo $\sigma-\pi$ hyperconjugation, leading to a shortening of the C—C bond.

Following this work, the study of surface ethylidyne emphasized questions other than its structural characterization. Creighton *et al.* used SSIMS to study the kinetics of H—D exchange into ethylidyne (20, 22), and were able to explain the data by a one-by-one, stepwise exchange process, proceeding via a concerted mechanism, as opposed to one in which the ethylidyne first dehydrogenates, and then picks up a deuterium atom. Their reasoning is based on EELS and TPD data which show that upon heating, the ethylidyne undergoes an irreversible dehydrogenation reaction. Therefore, a mechanism in which a hydrogen atom first leaves the $-\text{CH}_3$ moiety in ethylidyne is not a logical first step in the isotopic exchange since this dehydrogenation step is irreversible (22). The concerted mechanism which they proposed for H—D exchange involved ethylidene (>CHCH_3).

Ethylene hydrogenation experiments by Zaera and Somorjai (21) carried out above a saturated overlayer of ethylidyne on

Pt(111) have shown that ethylene hydrogenation proceeds independently of, and at a much faster rate than, the hydrogenation of surface ethylidyne. This model was advanced since the surface concentration of ^{14}C -labeled species derived from $^{14}\text{C}_2\text{H}_4$ does not change appreciably during the ethylene hydrogenation reaction when ^{12}C ethylene is used as a reactant gas. The role of the ethylidene species ($>\text{CHCH}_3$) as a hydrogenation transfer agent or "co-catalyst" in C_2H_4 hydrogenation was postulated (21).

Very recently, Koel *et al.* have shown by EELS that a saturation overlayer of ethylidyne on Rh(111) is unaffected by 1 atm of static D_2 at room temperature (24). Furthermore, they find that the rate of H—D exchange into ethylidyne is roughly proportional to the fraction of bare metal sites for coverage less than saturation. This presumably is related to the dissociation of D_2 or H_2 on empty metal sites prior to subsequent atomic exchange into ethylidyne.

In contrast to this large body of work on single crystals, there are relatively few reports of attempts to characterize ethylidyne on supported metals. In a recent NMR study of $\text{C}_2\text{H}_2 + \text{Pt}$ supported on alumina, no ethylidyne formation was detected at room temperature (27). The authors proposed a model involving a mixture of CCH_2 and HCCH surface species. Likewise, a recent Raman study of $\text{C}_2\text{H}_2 + \text{Rh}/\text{Al}_2\text{O}_3$ has concluded that the acetylene molecule bonds in a side-on fashion in a three-fold hollow site (28).

Very recently, Sheppard *et al.* (29, 30), have reinterpreted some older data of his own (31) and of Soma (32, 33) as being due to the ethylidyne species on Pt, Pd, and Rh supported on Al_2O_3 and SiO_2 . The previous assignment for the "dehydrogenated species" on these surfaces was MCHCHM . Soma has demonstrated (33) that at 195 K, this species is more resistant to hydrogenation by H_2 than is the π -bonded ethylene, and that the "dehydrogenated species" only makes up 20% of the adsorbed ethylene at this temperature.

This paper reports the first detailed measurements of the properties of ethylidyne produced from C_2H_4 or C_2H_2 on a supported metal system. These results open up an important new area in the body of ethylidyne literature, since they represent a bridge between single-crystal surface systems and the less ideal high-area catalytic surface systems. In the present communication we wish to show results in which both the ethylidyne formation and the subsequent H—D exchange into ethylidyne is spectroscopically monitored using IR methods. The high resolution and frequency accuracy of IR spectroscopy compared to EELS is a significant factor in this study.

II. EXPERIMENTAL

A. Sample Preparation

All measurements were made on Pd/ Al_2O_3 preparations (10% Pd) produced by impregnation of Degussa Al_2O_3 (100 m^2/g) with $\text{Pd}(\text{NO}_3)_2 \cdot 2\text{H}_2\text{O}$ and deposition of this mixture onto a CaF_2 sample plate. The unreduced deposit was placed in a stainless-steel IR cell, decomposed under vacuum at 450 K, and reduced in H_2 ($P = 400$ Torr) for 4 h at 450 K followed by outgassing at 475 K for 12 h. This procedure yields a Pd deposit containing 2.7×10^{-3} g Pd spread uniformly over half of the 5.07- cm^2 CaF_2 support plate. Details of this procedure and of the IR cell design may be found elsewhere (34–37). By using a half-plate design (35–37), studies of the pure Al_2O_3 sample can be made in the same cell along with studies of Pd/ Al_2O_3 . The stainless-steel ultrahigh vacuum system and sample cell has a base pressure of $\leq 1 \times 10^{-8}$ Torr.

B. Spectroscopic Measurements

All transmission infrared spectra were acquired using a purged Perkin-Elmer Model PE-783 infrared spectrophotometer and Model 3600 data acquisition station. A slit program yielding a maximum resolution of 5.4 cm^{-1} was employed, with data acquisition times ranging from 8 to 200 s/ cm^{-1} .

The accessible spectral range is 4000 to $\sim 1050\text{ cm}^{-1}$.

C. Gas Handling and Purification

H_2 and D_2 were obtained from Matheson in high-pressure cylinders; the H_2 at a purity of 99.9995%, the D_2 at 99.99% with a D atom percentage of 99.5%. The C_2H_4 was obtained from Matheson and transferred from a high-pressure cylinder to a glass bulb at a purity of 99.99%. The C_2D_4 was obtained from the MSD Company at an enrichment of 99 atom% D. Acetylene was prepared by reaction of water with calcium carbide and purified by vacuum line fractionation six times through a trap cooled to 177 K; this method has been shown to produce water-free acetylene (25).

III. RESULTS

A. Reaction of C_2H_4 with $\text{Pd}/\text{Al}_2\text{O}_3$ at 303 K

The spectral developments for the room-temperature addition of C_2H_4 to $\text{Pd}/\text{Al}_2\text{O}_3$ are shown in Fig. 1. The vibrational mode of moderate intensity at 1333 cm^{-1} increases in absorbance with exposure to ethylene and occurs at a frequency which we will show is characteristic of the methyl

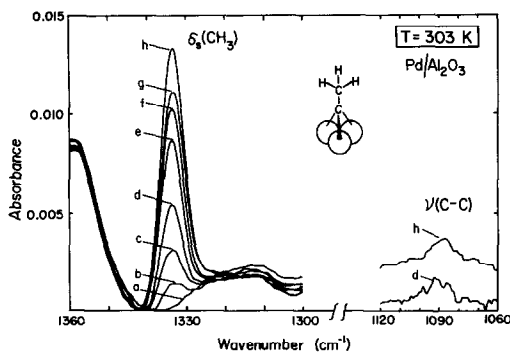


FIG. 1. Development of two IR modes for surface ethylidyne formed upon addition of C_2H_4 to $\text{Pd}/\text{Al}_2\text{O}_3$ at 303 K. The following numbers of C_2H_4 molecules have been adsorbed by the surface: (a) clean surface, (b) 0.20×10^{17} , (c) 0.54×10^{17} , (d) 0.96×10^{17} , (e) 1.50×10^{17} , (f) 2.26×10^{17} , (g) 2.93×10^{17} , (h) sample under vacuum, $P \leq 1 \times 10^{-6}$.

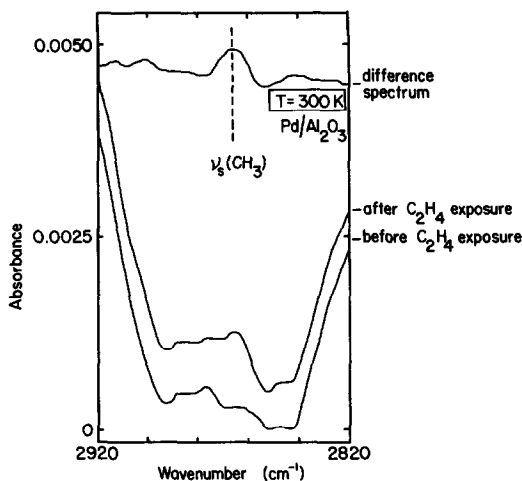


FIG. 2. Carbon-hydrogen stretching region for ethylidyne on $\text{Pd}/\text{Al}_2\text{O}_3$ following adsorption of $\approx 3 \times 10^{17}$ ethylene molecules.

group's symmetric deformation mode in adsorbed ethylidyne. The very weak band at 1088 cm^{-1} , shown at an intermediate and high ethylene exposure, will be shown to be characteristic of a C—C stretch in an sp^3 carbon. The invariant peak at 1360 cm^{-1} is a feature of the alumina support and is unrelated to the spectral changes which occur with increasing ethylene exposure.

The extremely weak band at 2867 cm^{-1} in Fig. 2 is due to the C—H stretch of an sp^3 -hybridized carbon atom. The top spectrum in Fig. 2 is the difference between the spectrum obtained at high ethylene exposures and that before any ethylene exposure. The sloping baseline which is removed as a result of taking a difference spectrum appears particularly large in this presentation due to the extreme scale expansion.

We will also show that the spectral feature at 1333 cm^{-1} is useful for studies of the reactivity of ethylidyne with other species. In particular, hydrogenation with either D_2 or H_2 causes this spectral feature to disappear. This process may be repeated many times by readsorption of C_2H_4 on the surface. The absorbance of the 1333-cm^{-1} feature is quantitatively reproduced in sequential experiments of this type.

B. Comparison of C_2H_2 and C_2H_4 Reaction with Pd/Al_2O_3 at 303 K

Acetylene, like ethylene, reacts with Pd/Al_2O_3 at room temperature, producing the same surface species as shown by the development of a methyl group deformation mode at 1329.5 cm^{-1} (Fig. 3). This acetylene-derived surface species differs from the ethylene-derived surface species in three respects:

(1) The acetylene-derived species exhibits a methyl group deformation mode frequency which is 3.5 cm^{-1} below that of the ethylene-derived species. This is shown in Fig. 3.

(2) The acetylene-derived peak at 1329.5 cm^{-1} maximizes in intensity at roughly half the peak intensity produced by a saturation ethylene exposure.

(3) Reaction of the surface species derived from both acetylene and ethylene with H_2 is rapid. Subsequent exposures of the surface to ethylene result in the development of the 1333-cm^{-1} mode to its full original intensity if prior exposures were made with ethylene, and *not acetylene*. That is, the initial exposure of a surface to acetylene results in decreasing the chemi-

sorption capacity of the sample for subsequent exposures to either C_2H_4 or C_2H_2 .

C. Thermal Development and Stability of the Ethylene-Derived Surface Species on Pd/Al_2O_3

Figure 4a–f shows the spectra for the supported Pd surface exposed to ethylene at temperatures between 150 and 302 K, and maintained in contact with a few tenths of a Torr of $C_2H_4(g)$ during warming. The C_2H_4 is either a liquid or gas, according to the sample temperature. At 150 K (Fig. 4a) the bands for $C_2H_4(l)$ are clearly seen at 1443 and 1341 cm^{-1} . Upon further warming to 198 K (Fig. 4b), these bands decrease in intensity as the $C_2H_4(l)$ evaporates, generating $C_2H_4(g)$, and presumably leaving behind a chemisorbed monolayer of C_2H_4 . The important feature, however, is the development of the characteristic 1333-cm^{-1} methyl group deformation mode at a temperature as low as 241 K (Fig. 4c), and quite clearly by 260 K (Fig. 4d), which continues in its development through 302 K (Figs. 4e,f).

When this same experiment is conducted in such a way as to remove all of the physisorbed ethylene at a temperature *below* that at which ethylidyne forms, the results are identical. This was done by exposing the clean Pd surface to excess $C_2H_4(g)$ at 150 K, and evacuating the sample at 150 K. By pumping on the sample during the warming process, we do not observe the bands at 1443 and 1341 cm^{-1} which are due to liquid ethylene. When the sample temperature is increased to $\sim 240\text{ K}$ under these conditions, the 1333-cm^{-1} band again develops as ethylidyne forms from adsorbed C_2H_4 .

Likewise, we have monitored the thermal stability of adsorbed ethylidyne at temperatures above room temperature. These results are shown in Figs. 4g–l, where it can be seen that the ethylidyne absorbance at 1333 cm^{-1} begins to attenuate at about 400 K indicating the onset of the decomposition of the surface species.

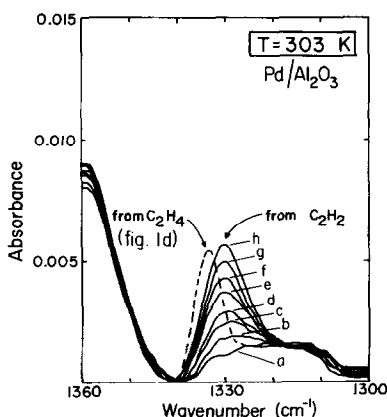


FIG. 3. Development of the "umbrella" mode for ethylidyne formation from C_2H_2 vs C_2H_4 . The following numbers of C_2H_2 molecules have been adsorbed by the surface: (a) 0.30×10^{17} , (b) 0.93×10^{17} , (c) 1.78×10^{17} , (d) 2.58×10^{17} , (e) 3.93×10^{17} , (f) 5.35×10^{17} , (g) 6.69×10^{17} , (h) 8.93×10^{17} .

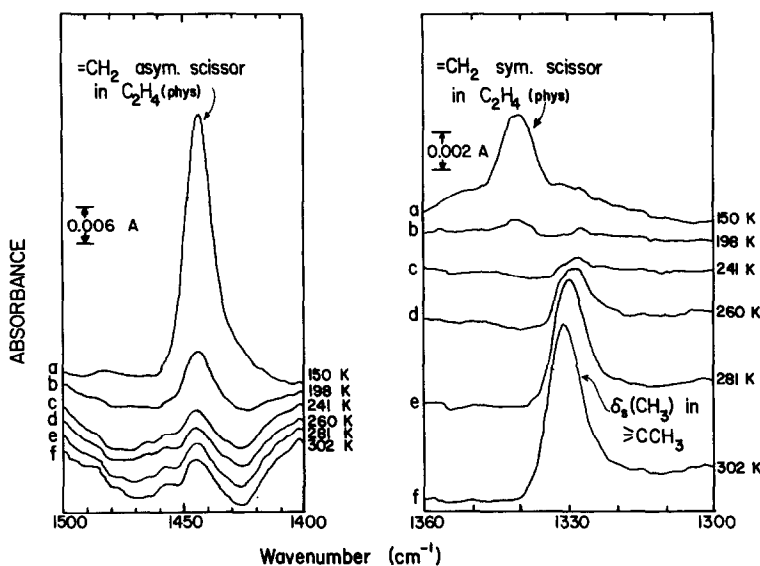


FIG. 4. Thermal development of ethylidyne on Pd/Al₂O₃ for $T = 150, 198, 241, 260, 281,$ and 302 K (spectra a through f, respectively), from the addition of C₂H₄. The sample was maintained under a few tenths of a Torr of C₂H₄(g) during the warming-up (spectra a–f). Spectra g through l are, in order, the spectra obtained at $T = 298, 350, 400, 450, 500,$ and 575 K.

D. Isotopic Studies: Addition of D₂ and C₂D₄ to Surface Ethylidyne

The experiment illustrated by the data in Fig. 5 was carried out by addition of small amounts of D₂(g) to a saturation coverage of the ethylene-derived surface species. Spectrum 5a clearly shows the two IR modes at 1333 and 1088 cm⁻¹. As greater amounts of D₂(g) are added (Figs. 5b–e), an absorption band at 1236 cm⁻¹ appears. The assignment of this new band will be discussed below. In addition, the 1333-cm⁻¹ band decreases in intensity monotonically, while the new, 1236-cm⁻¹ band maximizes in intensity before decreasing, with continued addition of D₂(g). The concomitant effects on the intensity of the $\nu(\text{C}-\text{C})$ band at 1088 cm⁻¹, as well as the possible growth of a band at ≈ 1120 cm⁻¹, is, unfortunately, not clear due to a signal-to-noise problem relating to the poor transmission of the CaF₂ windows and alumina support in this frequency range.

The data for the final experiment under-

taken is shown in Fig. 6. Starting from a saturation overlayer of the C₂H₄-derived surface species (Fig. 6a), and adding C₂D₄(g) to the pressures specified, we observe trends similar to those observed for the D₂ exchange experiment (compare Figs. 5 and 6) in which a peak develops at 1236 cm⁻¹. Some important differences do, however, exist. Since the experiments in Fig. 6 are being conducted under a pressure of C₂D₄(g), a sufficient excess of ethylene exists for the formation of the ethylidyne; the coverage of the surface species therefore, is constant, its deuterium content notwithstanding. Thus the peak at 1236 cm⁻¹ does not go through a maximum in intensity as it did with increasing exposure to D₂ in Fig. 5, but, rather increases in intensity as the 1333-cm⁻¹ peak decreases in intensity. In addition to the peak at 1236 cm⁻¹, Figs. 6b and c also show an IR band at 1120 cm⁻¹ which develops with the band at 1236 cm⁻¹. The assignments of these bands, as well as the reasons for the differences of the D₂ and C₂D₄ addition experiments will be discussed shortly.

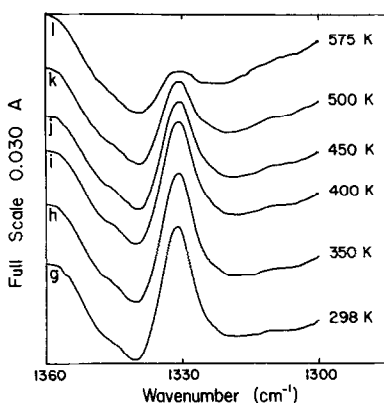


FIG. 4—Continued.

IV. DISCUSSION

A. Characterization of Surface Ethylidyne and Comparison with Results on Single Crystals

The data for the reaction of ethylene on Pd/Al₂O₃ to form a surface ethylene-derived species is shown in Figs. 1 and 2. The extensive body of characterizations of ethylidyne (\Rightarrow CCH₃) on various single-crystal metal surfaces makes it possible for us to compare the vibrational frequencies of ethylidyne on these surfaces to the fre-

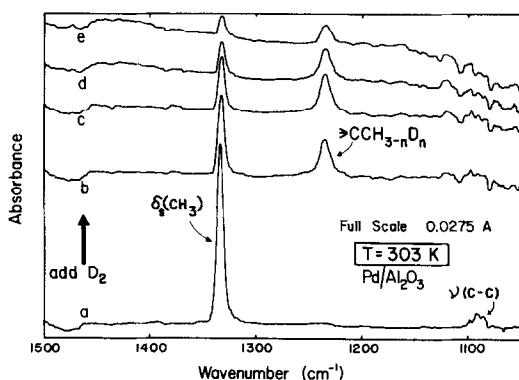


FIG. 5. Hydrogenation and isotopic exchange of D₂(g) into surface ethylidyne at $T = 303$ K. Spectra are difference spectra between clean surface and surface treated as follows: (a) addition of $\approx 3.3 \times 10^{17}$ molecules of C₂H₄ at 303 K. Spectra b through e are obtained from surfaces onto which the following additional amounts of D₂(g) has been adsorbed: (b) 1.5×10^{17} molecules, (c) 1.0×10^{17} molecules, (d) 5.0×10^{17} molecules, (e) 5.0×10^{17} molecules.

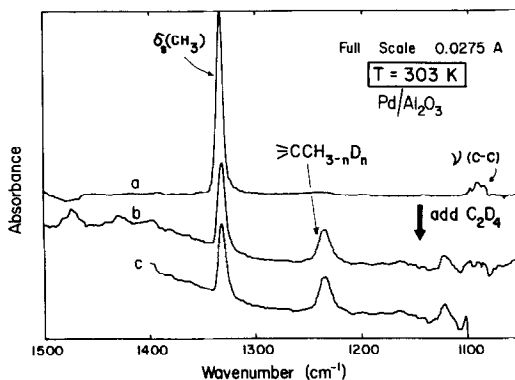


FIG. 6. Isotopic exchange of C₂D₄ into surface ethylidyne at $T = 303$ K. Spectra are difference spectra between clean surface and surface treated as follows: (a) addition of $\approx 3.3 \times 10^{17}$ molecules of C₂H₄ at (b) under a C₂D₄(g) pressure of 82×10^{-3} Torr, (c) under a C₂D₄(g) pressure of 134×10^{-3} Torr.

quencies of our ethylene-derived species. This comparison is shown in Table 1. The excellent agreement between our three observed frequencies and those for ethylidyne on the other surfaces, as well as the agreement with the cobalt organometallic complex allows us to make the assignment of surface ethylidyne for the species on the Pd/Al₂O₃ surface as shown in Table 1. The relative peak intensities also closely match the relative peak intensities in all the EELS data on single crystals and the relative peak intensities in the cobalt-ethylidyne complex. These correlations, as well as shifts in peak frequency upon deuteration (discussed below) allow us to assign the species to the ethylidyne structure. We have carefully looked in the regions where the infrared modes that are not of a_1 symmetry [$\nu_{as}(\text{CH}_3)$ and $\delta_{as}(\text{CH}_3)$] would be expected to appear. We have not observed any intensity in these frequency regions, consistent with the "surface selection rule" for adsorbates on metal surfaces, as discussed in the limit of small metal particle size by Greenler (39).

 B. Ethylidyne Formation from C₂H₂ vs C₂H₄

It can be seen in Fig. 3 that the reaction

TABLE I
Comparison of Vibrational Frequencies for Ethylidyne on Various Metal Surfaces (in cm^{-1})

Mode	Surface: Pt(111) ^a	Rh(111) ^b	Pd(111) ^c	Pd/Al ₂ O ₃ ^d	CH ₃ CCO ₃ (CO) ₉ ^e
ν_{as} (CH ₃)	3105–3025	2920	2900 (br.)	Not allowed	2930
ν_{s} (CH ₃)	2940–2900	2880		2867(v.w.)	2888
δ_{as} (CH ₃)	1420	1420	1400	Not allowed	1420
δ_{s} (CH ₃)	1350	1337	1334	1333(m)	1356
ν_{s} (C–C)	1130	1121	1080	1088(v.w.)	1163

^a Refs. (3, 4, 15).

^b Refs. (8, 24).

^c Refs. (12, 17, 19).

^d This work.

^e Ref. (11).

of C₂H₂ with Pd/Al₂O₃ leads to the development of a peak at 1329.5 cm^{-1} , 3.5 cm^{-1} lower than the ethylene-derived ethylidyne peak. Also evident in Fig. 3 is the early saturation of the surface with respect to formation of ethylidyne from acetylene. In addition, the surface after such exposure to C₂H₂ is relatively inactive toward regeneration with hydrogen at room temperature for the subsequent formation of ethylidyne. This is in contrast to a surface treated with C₂H₄, which regenerates very quickly and easily by exposure to a few Torr of H₂ at 300 K. The reaction of the surface ethylidyne with hydrogen to form ethane is rapid at 300 K, leaving a surface which is able to form more ethylidyne.

We explain all three effects on C₂H₂-derived surfaces, the 3.5- cm^{-1} shift, the early peak saturation, and the surface poisoning, by the following argument. The stoichiometry of the ethylidyne complex (C₂H₃) compared to that of gas-phase acetylene (C₂H₂) requires that for every 1 ethylidyne formed from acetylene, at least 2 acetylenes are required, due to the hydrogen deficiency of acetylene with respect to ethylidyne. An acetylene molecule which decomposes to give up its hydrogen(s) could be the source of a surface carbon or hydrocarbon fragment species which may cause all three of the above-mentioned effects. The early sur-

face saturation with respect to ethylidyne formation could arise from sites being blocked by the surface carbon or hydrocarbon fragment species. This species is apparently also unreactive to hydrogenation, accounting for the difficulty in regenerating the surface with hydrogen.

The shift of 3.5 cm^{-1} to lower wavenumber of the "umbrella" mode, δ_{s} (CH₃) could also be caused by weak interaction of acetylene-derived ethylidyne with a surface carbon or hydrocarbon fragment species. There is a precedent for these weak interaction effects in other systems. Yates and Haller (40) have observed small (5 to 8 cm^{-1}) shifts to lower wavenumber in vibrational frequencies for chemisorbed CO and N₂ when the chemisorbed molecule is surrounded by physisorbed species (CO, N₂, Xe) at low temperatures. There is additional evidence in the matrix isolation systems where so-called "matrix effects" attributed to neighboring molecules cause a small shift to lower wavenumber (41). There is some evidence that this is a general effect (40). In addition to purely physical "through-space" interaction, an electronic, through-metal interaction could also occur between surface species, and these possibilities are currently under study. The observation of this effect for C₂H₄ vs C₂H₂ in the ethylidyne system on single crystals has

not been reported since the state-of-the-art resolution in EELS is 30 cm^{-1} (13), while the uncertainty in the vibrational band frequencies from EELS is $\pm 5\text{ cm}^{-1}$ at best (42). Such a small shift of 3.5 cm^{-1} could not be seen by EELS as currently practiced.

C. Thermal Development and Stability of Ethylidyne

Figures 4a through f show the details of the developments upon warming the Pd/Al₂O₃ surface exposed to C₂H₄. At 150 K (Fig. 4a) a temperature at which C₂H₄ is in the liquid state, the prominent bands are those due to the CH₂ asymmetric scissoring motion of ethylene at 1443 cm^{-1} and the weaker, Raman-active band at 1340 cm^{-1} , due to a symmetric CH₂ scissoring motion. Upon warming to 198 K (Fig. 4b), all peaks decrease in intensity as the C₂H₄(l) converts to C₂H₄(g). Further warming to 241 K shows the first development of ethylidyne at 1329 cm^{-1} , which continues in its development through 302 K (Figs. 4c–f). Throughout the warming-up development of peaks, the sample is maintained in contact with a few tenths of a Torr of C₂H₄(g). We have found that this low pressure of C₂H₄(g) causes a negligible contribution to the spectra on this scale expansion. The onset of ethylidyne development at 241 K agrees with analogous experiments on Pd(111) where the onset of ethylidyne formation occurs between 150 and 300 K (12, 17).

By conducting the experiment in such a way as to remove all physisorbed C₂H₄ at a temperature below the ethylidyne formation temperature, the ethylidyne formation still proceeds to the same extent upon warming as that shown in Fig. 4f. This indicates that it is solely the first, or chemisorbed, layer of C₂H₄ which is involved in the formation of ethylidyne.

Likewise, spectra 4g–l show that the decomposition of surface ethylidyne begins at about 400 K in agreement with results on Pd(111) (12, 17). This decomposition is irre-

versible, and upon cooling and addition of more C₂H₄, little new ethylidyne forms. We feel that the surface may be poisoned by unreactive C_xH_y fragments formed at higher temperatures as the ethylidyne decomposes. Such fragments were reported by Gates and Kesmodel (17) on Pd(111). We have not, however, seen any evidence in the IR for such fragments, possibly because of the extremely weak intensity of these modes.

D. Isotopic Studies: Addition of D₂ and C₂D₄ to Surface Ethylidyne

Addition of D₂ to a saturated surface layer of ethylidyne causes the formation of the new band at 1236 cm^{-1} (see Fig. 5). Based on the frequencies observed and calculated (38) for ethylidyne on Rh(111) (see Table 2), this new peak could be either the CH₂ wag of $\geq\text{CCH}_2\text{D}$ or the CH rock of $\geq\text{CCHD}_2$ (1248 and 1239 cm^{-1} on Rh(111), respectively), or, less likely, a superposition of both. As can be seen from Table 2, the "umbrella" mode for the fully deuterated ethylidyne species ($\geq\text{CCD}_3$) occurs at a frequency just below our useful IR transmission range.

Recent SSIMS investigations of ethylidyne on Pt(111) (20, 22) have shown that incorporation of deuterium into the ethylidyne methyl group proceeds via a mechanism which agrees with a model of one-by-one stepwise exchange. In this model, the surface concentrations of intermediate deuteration species ($\geq\text{CCH}_{3-x}\text{D}_x$, $x = 1, 2$) go

TABLE 2

Vibrational Frequencies for Various Deuterated Ethylidynes on Rh(111) (in cm^{-1}) (38)

Mode	$\geq\text{CCH}_3$	$\geq\text{CCH}_2\text{D}$	$\geq\text{CCHD}_2$	$\geq\text{CCD}_3$
δ_s (CH ₃)	1337	<i>a</i>	<i>a</i>	988
ν (C–C)	1121	1125	1130	1145
CH ₂ wag	<i>a</i>	1248	<i>a</i>	<i>a</i>
γ (CH)	<i>a</i>	<i>a</i>	1239	<i>a</i>

^a Mode does not exist due to the symmetry of the species.

through a maximum with time as exchange of deuterium for hydrogen proceeds, while that of the undeuterated and fully deuterated species asymptotically fall and rise, respectively. The behavior of the 1236-cm^{-1} peak of our work does go through a maximum in intensity, probably due to the *competing* effects of stepwise exchange of D into the ethylidyne and the decreasing surface concentration of ethylidyne due to hydrogenation to ethane.

The hydrogenation effect is not a factor in Fig. 6 since the experiment is carried out under a pressure of C_2D_4 . Exchange possibly now proceeds as a result of C_2D_4 forming $\text{>CCD}_3 + \text{D(ads)}$ with involvement of an intermediate structure such as ethylidene, >CHCH_3 . Although we have no evidence for its formation, there is currently support for the ethylidene intermediate in this exchange process (20, 22, 24), and we are presently involved in experiments to help elucidate the mechanism.

The very weak new peak at 1120 cm^{-1} (Fig. 6) is most likely due to the C—C stretch mode in the mono- or dideuterated ethylidyne species, in agreement with results on Rh(111) (38) (see Table 2). Its presence is seen more easily in Fig. 6 than in Fig. 5 due to the lack of a competing hydrogenation reaction, which would cause a decrease in surface ethylidyne coverage.

V. SUMMARY

We report the first detailed investigation of the properties of ethylidyne on a supported metal surface ($\text{Pd/Al}_2\text{O}_3$, 10%). Its formation is immediate upon addition of C_2H_4 or C_2H_2 to $\text{Pd/Al}_2\text{O}_3$ at 303 K; the position of the IR bands are in excellent agreement with results obtained by EELS on Pd(111), Pt(111), and Rh(111) surfaces by others, and with the cobalt organometallic cluster compound containing ethylidyne. A small downward frequency shift of 3.5 cm^{-1} was observed for the "umbrella" mode of ethylidyne when it was formed from C_2H_2 , and this has been attributed to weak interaction of ethylidyne with a surface carbon

or hydrocarbon fragment species which is a product of the necessary decomposition of 2 acetylene molecules to form 1 ethylidyne species. The thermal characteristics of ethylidyne also agree with results on Pd(111), from the onset of its formation at $\approx 240\text{ K}$ upon warming from lower temperatures, to its decomposition beginning at about 400 K. Hydrogen–deuterium exchange into the ethylidyne molecule has also been studied with addition of $\text{D}_2(\text{g})$ and $\text{C}_2\text{D}_4(\text{g})$, with the observation that appreciable amounts of competing hydrogenation does occur with addition of $\text{D}_2(\text{g})$. The frequencies of the new bands resulting from incorporation of D into the ethylidyne molecule are in excellent agreement with those on Rh(111).

ACKNOWLEDGMENTS

The authors acknowledge with thanks the support of this work by the Science Research Laboratory and the 3M Central Research Laboratories. We also acknowledge helpful discussions with Dr. John Crowell, Professor Normal Sheppard, Dr. Allen Siedle, Mr. Kevin Uram, and Dr. Francisco Zaera.

REFERENCES

1. Kesmodel, L. L., Baetzold, R. C., and Somorjai, G. A., *Surf. Sci.* **66**, 299 (1977).
2. Demuth, J. E., *Chem. Phys. Lett.* **45**, 12 (1977).
3. Ibach, H., Hopster, H., and Sexton, B., *Appl. Surf. Sci.* **1**, 1 (1977).
4. Ibach, H., and Lehwald, S., *J. Vac. Sci. Technol.* **15**, 407 (1978).
5. Kesmodel, L. L., Dubois, L. H., and Somorjai, G. A., *Chem. Phys. Lett.* **56**, 267 (1978).
6. Kesmodel, L. L., Dubois, L. H., and Somorjai, G. A., *J. Chem. Phys.* **70**, 2180 (1979).
7. Demuth, J. E., *Surf. Sci.* **80**, 367 (1979).
8. Dubois, L. H., Castner, D. G., and Somorjai, G. A., *J. Chem. Phys.* **72**, 5234 (1980).
9. Anderson, A. B., and Hubbard, A. T., *Surf. Sci.* **99**, 384 (1980).
10. Baro, A. M., and Ibach, H., *J. Chem. Phys.* **74**, 4194 (1981).
11. Skinner, P., Howard, M. W., Oxton, I. A., Kettle, S. F. A., Powell, D. B., and Sheppard, N., *J. Chem. Soc. Faraday Trans. 2* **77**, 1203 (1981).
12. Kesmodel, L. L., and Gates, J. A., *Surf. Sci.* **111**, L747 (1981).
13. Ibach, H., and Mills, D. L., "Electron Energy

- Loss Spectroscopy and Surface Vibrations," pp. 326-335. Academic Press, New York, 1982.
14. Albert, M. R., Sneddon, L. G., Eberhardt, W., Greuter, F., Gustafsson, T., and Plummer, E. W., *Surf. Sci.* **120**, 19 (1982).
 15. Steininger, H., Ibach, H., and Lehwald, S., *Surf. Sci.* **117**, 685 (1982).
 16. Koestner, R. J., Van Hove, M. A., and Somorjai, G. A., *Surf. Sci.* **121**, 321 (1982).
 17. Gates, J. A., and Kesmodel, L. L., *Surf. Sci.* **124**, 68 (1983).
 18. Lloyd, D. R., and Netzer, F. P., *Surf. Sci.* **129**, L249 (1983).
 19. Kesmodel, L. L., and Gates, J. A., *J. Electron Spectrosc. Relat. Phenom.* **29**, 307 (1983).
 20. Creighton, J. R., and White, J. M., *Surf. Sci.* **129**, 327 (1983).
 21. Zaera, F., and Somorjai, G. A., *J. Amer. Chem. Soc.* **106**, 2288 (1984).
 22. Creighton, J. R., Ogle, K. M., and White, J. M., *Surf. Sci.* **138**, L137 (1984).
 23. Koestner, R. J., Stohr, J., Gland, J. L., and Horsley, J. A., *Chem. Phys. Lett.* **105**, 332 (1984).
 24. Koel, B. E., Bent, B. E., and Somorjai, G. A., *Surf. Sci.* **146**, 211 (1984).
 25. Albert, M. R., Ph.D. thesis. University of Pennsylvania, 1982.
 26. Salmeron, M., and Somorjai, G. A., *J. Phys. Chem.* **86**, 341 (1982).
 27. Wang, P. K., Slichter, C. P., and Sinfelt, J. H., *Phys. Rev. Lett.* **53**, 82 (1984).
 28. Parker, W. L., Siedle, A. R., and Hexter, R. M., *J. Amer. Chem. Soc.* **107**, 264 (1985).
 29. Sheppard, N., James, D. I., Lesiunas, A., and Prentice, J. D., *Commun. Dep. Chem. (Bulg. Acad. Sci.)* **17**, 95 (1984).
 30. Bandy, B. J., Chesters, M. A., James, D. I., McDougall, G. S., Pemble, M. E., and Sheppard, N., submitted for publication.
 31. Morrow, B. A., and Sheppard, N., *Proc. R. Soc. London Ser. A* **311**, 391 (1969).
 32. Soma, Y., *J. Chem. Soc. Chem. Commun.*, 1004 (1976).
 33. Soma, Y., *J. Catal.* **59**, 239 (1979).
 34. Yates, J. T., Jr., Duncan, T. M., and Vaughan, R. W., *J. Chem. Phys.* **71**, 3908 (1979).
 35. Wang, H. P., and Yates, J. T., Jr., *J. Phys. Chem.* **88**, 852 (1984).
 36. Gelin, P., Siedle, A. R., and Yates, J. T., Jr., *J. Phys. Chem.* **88**, 2978 (1984).
 37. Beebe, T. P., Jr., Gelin, P., and Yates, J. T., Jr., *Surf. Sci.* **148**, 526 (1984).
 38. Bent, B. E., private communication.
 39. Greenler, R. G., *J. Chem. Phys.* **44**, 310 (1966); **50**, 1963 (1969).
 40. Yates, J. T., Jr., and Haller, G. L., *J. Phys. Chem.* **88**, 4660 (1984).
 41. Hallam, H. E., Ed., "Vibrational Spectroscopy of Trapped Species." Wiley, London, 1973.
 42. Bell, A. T., and Hair, M. L., "Vibrational Spectroscopies for Adsorbed Species," p. 166. Amer. Chem. Soc., Washington, 1980.